Direct Simulation of Reed Wind Instruments

Article *in* Computer Music Journal · December 2009

DOI: 10.1162/comj.2009.33.4.43 · Source: DBLP

1 author:

Stefan Bilbao
The University of Edinburgh
182 PUBLICATIONS **1,882** CITATIONS

SEE PROFILE

DIRECT SIMULATION FOR REED WIND INSTRUMENTS

*Stefan Bilbao**

Music/Acoustics and Fluid Dynamics Group,
University of Edinburgh
Edinburgh, UK
sbilbao@staffmail.ed.ac.uk

1. INTRODUCTION

The synthesis of sound based on physical models of wind instruments has traditionally been carried out in a variety of ways. Digital waveguides [1, 2, 3, 4] have been extensively explored, especially in the special cases of cylindrical and conical tubes, in which case they yield an extreme efficiency advantage. A related scattering method, wave digital filtering [5], is also used in order to connect waveguide tube models with lumped elements such as an excitation mechanism [6] or toneholes [7]. Another body of techniques, closely related to digital waveguides, and based around impedance descriptions, has been developed recently [8]. Other techniques, employing finite difference approximations to the reed model (in opposition to wave- and scattering-based methods) bear a closer resemblance to the direct simulation methods to be discusssed here [9, 10, 11]. Most of these methods owe a great deal to the much earlier treatment of self-sustained musical oscillators due to McIntyre, Schumacher and Woodhouse [12].

All of these methods rely, to some degree, on simplified descriptions of the resonator (tube)—for example, digital waveguides make use of a traveling wave decomposition, accompanied by frequency-domain (impedance or reflectance) characterizations of lumped elements or phenomena such as bell radiation and tone holes. Other methods make use of the Green's function or impulse response of the tube directly [12]. These methods are, in the end, implemented in the time domain, but the notion of the spatial extent of the tube is suppressed—the system is viewed in an input-output sense. When it comes to sound synthesis, however, it is not clear that it is necessary to do so—once one has arrived at a satisfactory model of a musical instrument, written as a time-space PDE system (for the resonator) coupled to ODEs (the excitation element and a radiation boundary condition), one may proceed directly to a synthesis algorithm without invoking any notion of frequency, impedance, wave variables, or reflectance, or otherwise making any hypotheses about the dynamics of the air in the tube. Though one of course loses the powerful analysis perspective mentioned above, the treatment of the resonator becomes independent of any particular bore profile, and the system as a whole is now much more amenable to interesting extensions involving, e.g., time-varying and nonlinear effects which do indeed play a role in wind instruments, and which are not easily approached using impedance or scattering concepts.

In the present case, concerned with audio synthesis (and thus efficiency), the model remains 1D; standard numerical techniques, and in particular finite difference schemes have been applied (infrequently) to acoustic tube modeling for some time, especially in the case of speech synthesis—see, e.g., the recent paper by van den Doel and Ascher [13], and the much older but prescient and comprehensive treatment of Portnoff [14]. Finite difference schemes have also been applied in multi-D, in the setting of acoustical analysis of wind instruments, though generally not directly for synthesis—see. e.g., [15, 16].

A standard model of a reed wind instrument is presented in Section 2, followed by a development of a finite difference time domain algorithm in Section 3, including some discussion of implemntation details, such as the operation count, and computability issues. Connections to toneholes are introduced in Section 4. In Section 5, simulation results are presented.

This article appeared, in a modified form, at a recent conference [17], and also forms the basis for a section in a new text [18].

2. A STANDARD WIND INSTRUMENT MODEL

2.1. Instrument Body

A standard model of one-dimensional linear wave propagation in an acoustic tube [19] is given by the following set of equations:

$$\frac{\rho}{S}u_t = -p_x \qquad \frac{S}{\rho c^2}p_t = -u_x \qquad x \in [0, L] \tag{1}$$

Here, $u(x,t)$ and $p(x,t)$ are the volume velocity and pressure, respectively, at position x, and at time t, and subscripts t and x refer to time and space differentiation, respectively. ρ and c are the density and wave speed, respectively, $S(x)$ is the tube cross-sectional area[1] at position x, and L is the length of the tube. See Figure 1. The system above is often condensed into a single second order system, known as Webster's equation [21]:

$$S\Psi_{tt} = c^2 \left(S\Psi_x\right)_x \qquad x \in [0, L] \tag{2}$$

in terms of a velocity potential $\Psi(x,t)$, related to the pressure p and volume velocity u by $p = \rho\Psi_t$ and $u = -S\Psi_x$. Such an equation is the starting point for various speech synthesis algorithms [22], including the Kelly-Lochbaum model [23]. This model results from many simplifying assumptions, the most important of which are linearity, relatively slow variation in $S(x)$ and the size of $S(x)$ relative to audio wavelengths, and losslessness. For more comments on these assumptions (some more justifiable than others), see Section 6.

It is useful to dimensionally reduce the problem, by introducing the variables $x' = x/L$, $\Psi' = \Psi/cL$, as well as a dimensionless area function $S' = S/S_0$, where S_0 is a reference surface

* This work was supported by the Engineering and Physical Sciences Council UK, under grant number C007328/1, the Leverhulme Trust, and the CONSONNES project.

[1] Or, rather, the area of an isophase surface of the pressure distribution in the tube [20].

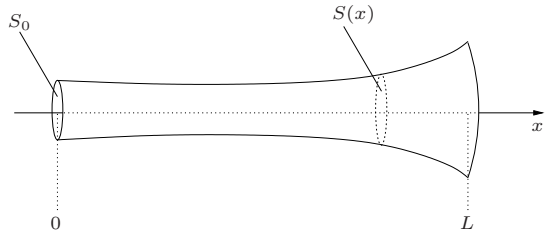

Figure 1: *Acoustic tube of variable cross-sectional area* $S(x)$

area, such as $S_0 = S(x = 0)$. This leads, after substitution in (1) and removal of primes, to

$$S\Psi_{tt} = \gamma^2 \left(S\Psi_x\right)_x \qquad x \in [0, 1] \tag{3}$$

where $\gamma = c/L$ is a constant with dimensions of frequency. Initial conditions for the system may be set to zero, and proper boundary conditions (one required at each end of the domain) follow from the consideration of the reed excitation and bell radiation, to be discussed shortly.

2.2. Reed Mechanism

A slightly non-standard model of reed vibration may be given as follows (see Figure 2). For a one-mass model, the reed displacement behaves according to

$$\ddot{y} + 2\sigma_0\dot{y} + \omega_0^2(y - H_0) - \frac{\omega_1^{\alpha+1}}{H_0^{\alpha-1}}\left(|[y]^-|\right)^\alpha = -\frac{S_\mathrm{r} p_\Delta}{M_\mathrm{r}} \tag{4}$$

$y(t)$ is here the displacement of the reed relative to an equilibrium position y_0, S_r an effective surface area of the reed, M_r is the reed mass, ω_0 the resonant frequency, and σ_0 a damping parameter. Dots above variables signify total time differentiation. The term involving the coefficient ω_1 models the collision of the reed with the mouthpiece. It acts as a one-sided repelling force, modelled as a power-law nonlinearity, of exponent α, and becomes active when $y < 0$. Here, $[y]^- = (y - |y|)/2$ and the reed displacement y is permitted to be negative. This term, inspired by collision models used in hammer-string dynamics [24], is the sole distinguishing feature of the model, which is otherwise identical to that which appears in the literature [25, 26, 27, 28, 11].

The oscillator above is driven by the pressure difference p_Δ, given by

$$p_\Delta = p_\mathrm{m} - p_\mathrm{in}$$

where $p_\mathrm{m}(t)$ is the mouth pressure, and $p_\mathrm{in}(t)$ the pressure at the entrance to the acoustic tube. Through Bernoulli's law, the pressure difference may be related to the flow in the mouthpiece u_m by

$$u_\mathrm{m} = w[y]^+\sqrt{\frac{2|p_\Delta|}{\rho}}\mathrm{sign}(p_\Delta) \tag{5}$$

where here, w is the width of the reed channel. The flow is nonzero only when the reed is not in contact with the mouthpiece, or when $y > 0$. As such, the quantity $[y]^+$ is given by $[y]^+ = (y + |y|)/2$. Neglected here is an inertia term—see, e.g., [21]. From a numerical standpoint, the square root dependence of flow on velocity could be generalized to a power law [29] with few resulting complications in the discretization procedure to be outlined below.

The flow variables are related by a conservation law

$$u_\mathrm{in} = u_\mathrm{m} - u_\mathrm{r}$$

where u_in is the flow entering the acoustic tube, and where u_r is related to reed displacement y by

$$u_r = S_\mathrm{r}\dot{y}$$

It is useful to introduce scaled variables as follows:

$$y' = \frac{y}{H_0} - 1 \qquad p_\cdot' = \frac{p_\cdot}{\rho c^2} \qquad u_\cdot' = \frac{u_\cdot}{cS_0}$$

Here, $p_\cdot$ and $u_\cdot$ indicate any pressure or flow variables, which, when inserted in the above equations (and primes subsequently removed) lead to the system:

$$\begin{aligned}
\ddot{y} + 2\sigma_0\dot{y} + \omega_0^2 y &= -\mathcal{Q}p_\Delta + \omega_1^{\alpha+1}\left(|[y+1]^-|\right)^\alpha && \text{(6a)}\\
p_\Delta &= p_\mathrm{m} - p_\mathrm{in} && \text{(6b)}\\
u_\mathrm{m} &= \mathcal{R}[y+1]^+\sqrt{|p_\Delta|}\mathrm{sign}(p_\Delta) && \text{(6c)}\\
u_\mathrm{in} &= u_\mathrm{m} - u_\mathrm{r} && \text{(6d)}\\
u_\mathrm{r} &= \mathcal{S}\dot{y} && \text{(6e)}
\end{aligned}$$

where

$$\mathcal{Q} = \frac{\rho c^2 S_\mathrm{r}}{M_\mathrm{r} H_0} \qquad \mathcal{R} = \sqrt{2}\frac{wH_0}{S_0} \qquad \mathcal{S} = \frac{S_\mathrm{r} H_0}{cS_0} \tag{7}$$

Note that higher-order effects of the time variation of H_0 (which is possible during play), which is generally quite slow, are neglected here, as in previous treatments of the reed system [25]. Slow variation in H_0 may be introduced here through a function $H_0(t)$—notice that it affects all of the parameters $\mathcal{Q}$, $\mathcal{R}$ and $\mathcal{S}$.

It should be clear that in a connection with the acoustic tube described by (3), it must be true that

$$\Psi_t(0, t) = \gamma p_\mathrm{in}(t) \qquad \Psi_x(0, t) = -u_\mathrm{in}(t) \tag{8}$$

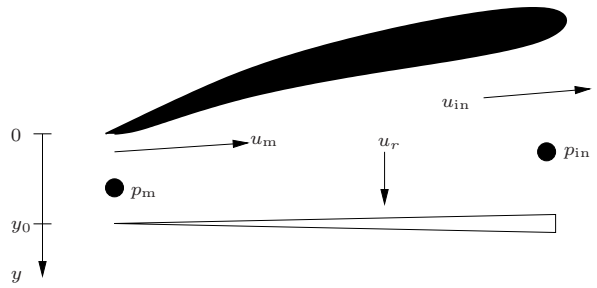

Figure 2: *Pressure and flow variables in a reed instrument mouthpiece.*

2.3. Bell Radiation

One boundary condition is required for Webster's equation (3) at the bell termination at $x = 1$. Normally, in the musical acoustics literature (see, e.g., [21, 30]), one employs the standard radiation impedance result for an unflanged tube. Often, this is given, in the low-frequency limit, in a polynomial form obtained through

a series approximation [30, 21]. While this is fine for analysis purposes, positive realness [31] (and thus passivity) is lost, and numerical instabilities can arise in simulation. It is thus better, in this context, to make use of a rational and positive real approximation to the radiation impedance (see, e.g., the form given in [22]), leading to the following relationship between scaled pressure and velocity at $x = 1$:

$$\Psi_x(1,t) = -\alpha_1 \Psi_t(1,t) - \alpha_2 \Psi(1,t) \tag{9}$$

In the case of an unflanged tube, the constants α_1 and α_2 take on the values:

$$\alpha_1 = \frac{1}{4(0.6133)^2\gamma} \qquad \alpha_2 = \frac{L}{0.6133\sqrt{S_0 S(1)/\pi}} \tag{10}$$

The term with coefficient α_2 corresponds to the reactive part of the radiation impedance, and that with coefficient α_1 to the resistive part. One could go much further here, and develop boundary conditions which model radiation to higher accuracy (thus requiring more state), but the positive realness criterion must continue to be enforced (i.e., a higher order polynomial series approximation to the radiation impedance will lead to the potential for active behaviour, and thus numerical instability in simulation). Positive realness of an impedance corresponds directly to bounded realness for the associated reflectance, a quantity which is probably better known to musical acousticians.

3. A SIMPLE FINITE DIFFERENCE SCHEME

There are many possible choices of finite difference scheme for Webster's equation, but, interestingly, the simplest possible choice is, in almost all respects, the best—see Section 3.1. A grid function Ψ_l^n for integer l, with $0 \leq l \leq N$, and $n \geq 0$, is an approximation to $\Psi(x,t)$ at locations $(x = lh, t = nk)$, where h and k are the spacing between adjacent grid points and time step, respectively. See Figure 3. k is related to the sample rate f_s by $k = 1/f_s$—in audio synthesis applications, k is normally chosen a priori. A simple scheme is of the following form:

$$\Psi_l^{n+1} = m_l^{(-)} \Psi_{l-1}^n + m_l^{(0)} \Psi_l^n + m_l^{(+)} \Psi_{l+1}^n - \Psi_l^{n-1} \tag{11}$$

where the Courant number λ is defined as $\lambda = k\gamma/h$, and where the scheme coefficients are given by

$$\begin{aligned} m_l^{(-)} &= \frac{2\lambda^2 (S_l + S_{l-1})}{S_{l-1} + 2S_l + S_{l+1}} \\ m_l^{(0)} &= 2 - 2\lambda^2 \\ m_l^{(+)} &= \frac{2\lambda^2 (S_l + S_{l+1})}{S_{l-1} + 2S_l + S_{l+1}} \end{aligned}$$

where $S_l \triangleq S(lh)$, and where λ, the Courant number, is given by $\lambda = \gamma k/h$. In implementation, the coefficients above may be precomputed, with minimal effort.

A necessary condition for numerical stability is

$$\lambda \leq 1 \tag{12}$$

This is the familiar Courant-Friedrichs-Lewy condition [32, 33], arrived at through energy techniques (and not frequency or von Neumann analysis, which is not generally applicable to problems with spatial variation [18])—note that the condition is independent of the variation in S itself, simplifying implementation somewhat. In particular, for a given time step k, it is easiest to choose the grid spacing h so as to divide the unit interval into an integer number N of parts, and it is also important that (12) be satisfied as near to equality as possibility. This leads to the choice

$$N = \text{floor}\,(1/\gamma k) \qquad h = 1/N$$

Notice that one could choose a smaller value for N, leading, apparently, to reduced computational costs (i.e., fewer grid values must be computed). Such a choice, though it has been made by some in the context of speech synthesis (see, e.g., [13]), leads to severe dispersion, and bandlimiting of the output. See Section 3.1 for more on this.

The updating of Ψ, according to (11) necessarily requires a boundary condition at either end—these settings will be discussed shortly.

Scheme (11) may be shown to be equivalent to scattering forms commonly encountered in physical modeling sound synthesis—when $\lambda = 1$, it reduces to the Kelly-Lochbaum model, and if, furthermore, S is constant, it reduces further to the digital waveguide. See [18] for more details.

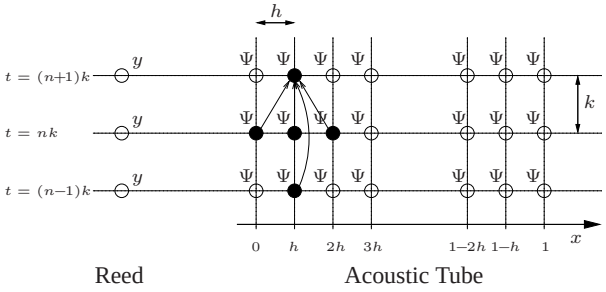

Figure 3: *Computational grid for finite difference scheme* (11) *for Webster's equation, coupled to a reed mechanism. At an interior point, the computational dependency of the scheme at a given grid point is indicated by the set of black points with accompanying arrows.*

3.1. Dispersion, Accuracy and Mode Tunings

Before proceeding to the case of a complete wind instrument, it is worth taking a look at the behaviour of scheme (11) on its own, especially with regard to the important issue of accuracy.

Scheme (11) is formally second-order accurate; one might assume, then, that numerical dispersion (and thus misplacement of modal frequencies) will be a major concern [32], as it can be for simulations for other systems in musical acoustics (such as, e.g., the transverse vibration of bars [18]). In fact, though, the formal order of accuracy only refers to the behaviour of the scheme in the low-frequency limit; the accuracy of the scheme is extremely good, over the whole range of audio frequencies, even for relatively exotic choices of the bore profile. Consider, for example, the case of the tube terminated by a zero-velocity condition at $x = 0$, and a zero-pressure condition at $x = 1$ (corresponding, roughtly, to a wind instrument configuration). One finds, using scheme (11), that the modal frequencies of the tube converge very rapidly to their exact values, so that even at a typical audio sample rate (such

as 44.1 kHz), the error is far below the threshhold of human audio perception—see Figure 4 for some typical values.

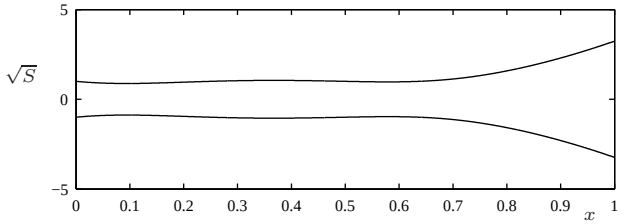

Mode #	Exact Freq. (Hz)	Scheme (11) Freq. (Hz)	Cent Dev.
1	194.17	194.21	0.34
2	550.89	550.69	-0.63
3	788.08	787.78	-0.65
4	1068.67	1068.50	-0.28
12	3456.35	3455.33	-0.51

Figure 4: *A tube profile, and comparisons between exact and numerical modal frequencies resulting from the use of scheme* (11)*, running at* 44.1 kHz*, and for a value of* λ *chosen as close to* 1 *as possible. At top, a tube profile grossly characteristic of a wind instruments with a value of* $\gamma = 600$*. A zero-velocity (Neumann) condition is used at the tube's left end, and a zero-pressure (Dirichlet) condition at its right end.*

In mainstream applications, better accuracy is obtained by using more involved differnce approximations. In the case of Webster's equation, however, higher-order accurate approximations will tend to degrade accuracy. The explanation of this apparent paradox is that the discretization errors in the temporal and spatial second-order approximations in (11) lead to a rather delicate cancellation—for much more on this topic, see the literature on so-called modified equation methods [34].

Some comments are in order in this point—first, in order to obtain this very accurate behaviour, the condition (12) must be satisfied as close to equality as possible. This means choosing the number of grid points N as large as possible. From the point of view of computational complexity, one must thus be wary of the temptation to choose a smaller N, to save on the total operation count—if one does, numerical dispersion, and, what is worse, a severe bandlimiting of the resulting audio output will result (see, e.g., the results shown in [13], where even at an audio sample rate, the output is bandlimited to far below the Nyquist. The issue of truncation is a distinction between difference methods and scattering methods such as waveguides—waveguides under truncation exhibit a slight detuning of modal frequencies, which may be corrected with recourse to fractional delay filters [35]; difference schemes do not exhibit this detuning, but rather a loss of bandwidth, which is typically very small if the stability condition is satisfied near equality (at 44.1 kHz, in a worst-case csenario for wind instruments, output is bandlimited to approximately 20 kHz).

3.2. Scheme for Reed System

For the reed system, given in (6), consider the following scheme:

$$\begin{aligned}
&\frac{1}{k^2}\left(y^{n+1}-2y^n+y^{n-1}\right)+\frac{\sigma_0}{k}\left(y^{n+1}-y^{n-1}\right)\\
&\quad+\frac{\omega_0^2}{2}\left(y^{n+1}+y^{n-1}\right) &\text{(13a)}\\
&\quad+\frac{\omega_1^{\alpha+1}}{2}|[y^n+1]^-|^{\alpha-1}\left(y^{n+1}+y^{n-1}\right)=-\mathcal{Q}p_\Delta^n\\
p_\Delta^n &= p_{\rm m}^n-p_{\rm in}^n &\text{(13b)}\\
u_{\rm m}^n &= \mathcal{R}[y^n+1]^+\sqrt{|p_\Delta^n|}\,\mathrm{sign}(p_\Delta^n) &\text{(13c)}\\
u_{\rm in}^n &= u_{\rm m}^n-u_{\rm r}^n &\text{(13d)}\\
u_{\rm r}^n &= \frac{\mathcal{S}}{2k}\left(y^{n+1}-y^{n-1}\right) &\text{(13e)}
\end{aligned}$$

Here, the functions y, $u_{\rm m}$, $u_{\rm r}$, $u_{\rm in}$, $p_{\rm m}$, $p_{\rm in}$, and p_Δ have been approximated by time series, with time step k. $p_{\rm m}$, in particular, is assumed to be a known input control signal, and $p_{\rm in}$ and $u_{\rm in}$ will be related to values of the grid function Ψ over the problem interior. Worth noting here is the approximation to the stiffness term (with coefficient ω_0^2) and the collision term (with coefficient $\omega_1^{\alpha+1}$), both of which make use of semi-implicit discretizations. Such implicit approximations, when applied to lumped systems such as the reed, significantly ease stability requirements, and, as long as the unknown value of the grid function appears linearly (as it does here) still allow for fully explicit updating—see Section 3.5.

3.3. Numerical Coupling to Reed System

In order to couple scheme (11) to the scheme (13) for the reed, numerical boundary conditions corresponding to the conditions (8) are necessary; here are particularly well-behaved choices:

$$p_{\rm in}^n=\frac{1}{2\gamma k}\left(\Psi_0^{n+1}-\Psi_0^{n-1}\right)\qquad u_{\rm in}^n=-\frac{1}{2h}\left(\Psi_1^n-\Psi_{-1}^n\right) \tag{14}$$

The second condition refers to a value of the grid function Ψ_l at a virtual location $l=-1$.

After some algebra, the system (13) above may be reduced to

$$\Delta p^n+a_1^n\sqrt{|\Delta p^n|}\mathrm{sign}\left(\Delta p^n\right)+a_2^n=a_3^n u_{\rm in}^n \tag{15}$$

where the coefficients $a_1^n\geq 0$, a_2^n and $a_3^n\geq 0$ will depend on known (previously computed) values of y^n and the various defining parameters of the reed system. (The non-negativity of a_1^n and a_3^n, follows from the use of semi-implicit discretizations to the stiffness terms.)

Using conditions (14), and the update (11), as well as (13b), one may arrive at the relation

$$p_\Delta^n=b_1^n-b_2^n u_{\rm in}^n \tag{16}$$

where again, b_1^n and $b_2^n\geq 0$ depend on previously computed values of the grid functions p and u, as well as the input pressure $p_{\rm m}$. Now, (15) and (16) may be combined into a single equation for the pressure difference p_Δ^n:

$$|p_\Delta^n|+c_1^n\sqrt{|p_\Delta^n|}+\frac{c_2^n}{\mathrm{sign}\left(p_\Delta^n\right)}=0 \tag{17}$$

for the coefficents $c_1^n \geq 0$ and c_2^n. One may then observe that, in order for a solution to exist, one must have $\text{sign}\,(p_\Delta^n) = -\text{sign}\,(c_2^n)$, at which point the magnitude $|p_\Delta^n|$ may be determined uniquely. In this case, due to the form of the pressure-flow characteristic (5), this may be done using the quadratic formula, but a unique solution will exist for any such characteristic which is one-to-one, though an iterative method (necessarily convergent) may be necessary. In this sense, finite difference updating is simpler here than in the closely related case of the bow-string interaction (in which case the nonlinear force-velocity characteristic is not necessarily one-to-one) [18].

3.4. Numerical Radiation Condition

For the scheme at the radiating termination, a discrete condition corresponding to (9) is

$$\begin{aligned}\frac{1}{2h}\left(\Psi_{N+1}^n - \Psi_{N-1}^n\right) &= -\frac{\alpha_1}{2k}\left(\Psi_N^{n+1} - \Psi_N^{n-1}\right) \\ &\quad -\frac{\alpha_2}{2}\left(\Psi_N^{n+1} + \Psi_N^{n-1}\right)\end{aligned}$$

When this condition is employed in scheme (11), the following specialized recursion at the boundary point at $l = N$ results:

$$\Psi_N^{n+1} = m_N^{(-)}\Psi_{N-1}^n + m_N^{(0)}\Psi_N^n + q_N\Psi_N^{n-1} \qquad (18)$$

where

$$\begin{aligned}m_N^{(-)} &= \frac{\lambda^2}{2\tau}\left(S_{N+1} + 2S_N + S_{N-1}\right) \\ m_N^{(0)} &= \frac{1}{\tau}\left(2 - \frac{\lambda^2}{2}\left(S_{N+1} + 2S_N + S_{N-1}\right)\right) \\ q_N &= \frac{1}{\tau}\left(\frac{\gamma^2 k^2}{2h}\left(S_{N+1} + S_N\right)\left(\frac{\alpha_1}{k} - \alpha_2\right) - 1\right)\end{aligned}$$

and where

$$\tau = \frac{\gamma^2 k^2}{2h}\left(S_{N+1} + S_N\right)\left(\frac{\alpha_1}{k} + \alpha_2\right) + 1$$

3.5. Explicit Updating

It is important to point out that, despite the apparently complex relationship among the stored variables at the terminations and the grid function to be updated over the interior, a purely explicit update form may be arrived at, but the order in which operations are performed is of great importance. Consider the entire scheme at the end of an update cycle, at which point all values at time step n or previously are known. One may then proceed as follows:

- Calculate p_Δ^n through the solution of (17)
- Calculate y^{n+1} through (13a)
- Calculate p_{in}^n using (13b) and the known value of p_{m}^n
- Calculate $\delta_{t\cdot}\Psi_0^n$, and thus Ψ_0^{n+1} using the first of the boundary conditions (14).
- Calculate the remaining values of Ψ_l^{n+1}, $l > 0$ using scheme (11) and (18).

At this point the updating cycle is complete, and the procedure may be repeated. Proponents of wave digital filtering often call attention to this computability issue, usually dealt with using so-called reflection-free ports [5]. One may see here that the same property is available using finite difference schemes, and furthermore, numerical solution uniqueness may be ensured (in contrast with wave digital methods making use of nonlinear elements, and power-normalized waves [36], where implicit solvers will be necessary).

3.6. Numerical Stability

The question of numerical stability of the simulation as a whole is a very delicate one. One may prove, using energy techniques [18], that in the absence of the reed model, the scheme (11), coupled with the numerical radiation boundary condition (14) is numerically stable, as long as condition (12) is satisfied.

When the reed model is introduced, however, the situation becomes much more complicated—though for many types of nonlinear systems, including schemes for bow-string interactions, and for nonlinear vibrations of strings and plates, one may develop solid stability conditions, the reed system presents some difficulties. The problem is the following: as a starting point, one would like to be able to bound some measure of the size of the state of the continuous model system (i.e., the reed coupled to the bore) in terms of the input signal $p_m(t)$. This is a natural requirement, and one which, in this case, is not met—it is difficult to show that there do not exist bounded input signals which are capable of producing unbounded output. This indicates the possibility that model of reed vibration presented here may not be fully correct, from an energetic standpoint. As such, it may not be possible to find a stability condition for the derived numerical scheme. On the other hand, it is rather difficult to actually exhibit any instability in the scheme proposed here—the author has tried, using the most perverse settings imaginable for the system parameters and input signal!

3.7. Computational Considerations

The computational cost of this algorithm is almost entirely due to the updating of the scheme for the tube, and, as such, is governed by the choice of time step k and grid spacing h, which are related by the CFL condition (12). The condition should be fulfilled as close to equality as possible—otherwise, as mentioned above, excessive numerical dispersion, leading to mode mistuning and a severe limitation in audio bandwidth [18] will result. Thus, for a given time step $k = 1/f_s$, the memory requirement will be almost exactly $2f_s/\gamma = 2f_sL/c$ units. Updating at a single grid point requires three arithmetic operations, and thus the total operation count will be $6f_s^2/\gamma = 6Lf_s^2/c$ operations/second. For typical wind instruments, and at a suitably high audio sample rate, such as $f_s = 44100$ Hz, the operation count will be on the order of tens of megaoperations/second, well within real time capability on a modest laptop computer. For example, on the author's laptop, a Dell with a 2.0 GHz Pentium, and for the case of a clarinet geometry, it takes approximately 3.9 s to generate 5 s of sound output, at 44.1 kHz, in Matlab—and sluggish Matlab code generally runs between 10 and 100 times slower than a standard C implemntation. On the other hand, an FD implementation is more expensive, in terms of arithmetic (though not memory) than a typical waveguide algorithm.

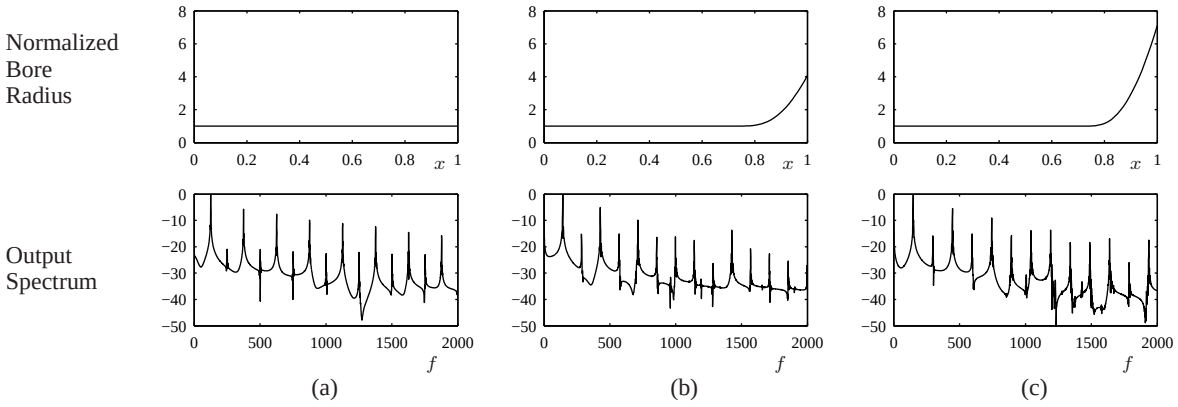

Figure 5: *Typical output spectra, for various bore types: (a) a cylinder, (b) a cylinder with a clarinet-like bell, and (c) a cylinder with a bell of extreme flare. In each case, the other model parameters correspond, roughly, to those of a clarinet:* $\gamma = 512$, $\mathcal{Q} = 1.6 \times 10^{10}$, $\mathcal{R} = 0.032$, $\mathcal{S} = 10^{-6}$, $\omega_0 = 23250$, $g = 3000$. *Scheme* (11) *is used, at a sample rate of 44.1 kHz.*

4. TONEHOLE MODELING

In the literature, the tonehole is ususally modelled as a branched side-tube, characterized as a two- or three-port lumped circuit element—the reader is referred to the ample literature on this subject, e.g., [37, 38]. Normally such an element is described in terms of series and shunt impedances, which depend on the hole radius and effective tonehole height (which depends on the state of the hole), and the enclosed volume.

It is, of course, possible to describe the behaviour of such an element directly in the time-space domain, by adding extra terms to Webster's equation. Here is one very simple variety, written in terms of dimensionless variables, which is equivalent to the lossless form given in [7]:

$$S\Psi_{tt} = \gamma^2 \left(S\Psi_x\right)_x - \delta(x - x_\mathrm{T})g \tag{19a}$$

$$g = \frac{\phi\gamma^2 S_\mathrm{T}}{\xi_\mathrm{e}}\Psi(x_\mathrm{T}) + (1-\phi)\xi S_\mathrm{T}\Psi_{tt}(x_\mathrm{T}) \tag{19b}$$

Here, ξ is the dimensionless ratio of the tonehole height to the tube physical tube length L, and S_T is the dimensionless ratio of the tonehole cross-sectional area to the area of the bore at its left end (not at the hole!). ϕ is a parameter which indicates the state of tonehole, ranging between $\phi = 0$ (closed) and $\phi = 1$ (open). The various forms for ξ, which depend on whether the hole is opened or closed, are effective lengths, and exact expressions appear in various publications [37, 39, 7]. In fact, the effective lengths themselves are frequency-dependent to a slight degree—such frequency dependence, as well as loss due to radiation [40] is ignored here, for the sake of simplicity (but can easily be reintroduced [18]). The lumped variable $g = g(t)$ is a variable used to store the additional state of the tonehole.

The model above is simplified from the usual form seen in the literature [37], which, when viewed as a two-port lumped circuit element, contains negative impedances (leading to the so-called negative length correction). Such negative elements can indeed be incorporated into the framework above [18], but at the risk of introducing numerically unstable behaviour, which is not surprising, given that such elements cannot be interpreted as passive.

In an FD implemntation, the coupling with the tone hole model may carried out using some form of interpolation (i.e., the tonehole location will not, in general, fall directly at one of the grid locations). Here is a general form:

$$\begin{aligned}\Psi_l^{n+1} &= m_l^{(-)}\Psi_{l-1}^n + m_l^{(0)}\Psi_l^n + m_l^{(+)}\Psi_{l+1}^n - \Psi_l^{n-1} \\ &\quad - \frac{4k^2}{S_{l-1} + 2S_l + S_{l+1}} J_l(x_\mathrm{T}) g^n \\ g^n &= \frac{\phi\gamma^2 S_\mathrm{T}}{2\xi_\mathrm{e}}\left(\Psi^{n+1}(x_\mathrm{T}) + \Psi^{n-1}(x_\mathrm{T})\right) \\ &\quad + \frac{(1-\phi)\xi S_\mathrm{T}}{k^2}\left(\Psi^{n+1}(x_\mathrm{T}) - 2\Psi^n(x_\mathrm{T}) + \Psi^{n-1}(x_\mathrm{T})\right)\end{aligned}$$

Here, $\Psi^n(x_\mathrm{T})$ is an interpolated value drawn from the grid function Ψ_l^n; if linear interpolation is used, for example, $\Psi^n(x_\mathrm{T}) = \alpha\Psi_{l_\mathrm{T}}^n + (1-\alpha)\Psi_{l_\mathrm{T}+1}^n$, where the interpolation point x_T lies between the grid locations $l = l_\mathrm{T}$ and $l = l_\mathrm{T} + 1$, and where $0 \leq \alpha < 1$ is an interpolation index. Similarly, the grid function $J_l(x_\mathrm{T})$ is an approximation to a delta function centered at x_T, and when linear interpolation is used, takes on the values $J_{l_\mathrm{T}} = \alpha/h$, $J_{l_\mathrm{T}+1} = (1-\alpha)/h$, and is zero otherwise.

Obviously, the interpolation and delta function approximation could be extended to a higher order, but linear approximation is probably sufficient. Interestingly, if the interpolation and delta function approximation are of the same order, one may prove numerical stability of the combined tube/tonehole system, under static conditions [18].

Though the scheme above apparently is implicit, it is possible to arrive at an explicit update, much in the same way as for the radiation termination [18].

5. SIMULATION RESULTS

This FD model successfully replicates many features of acoustic reed wind instruments (and also of other synthesis methods), and a variety of such features are presented here. Sound examples are available at the author's website, at

`http://ccrma.stanford.edu/~bilbao/soundex/reed/`

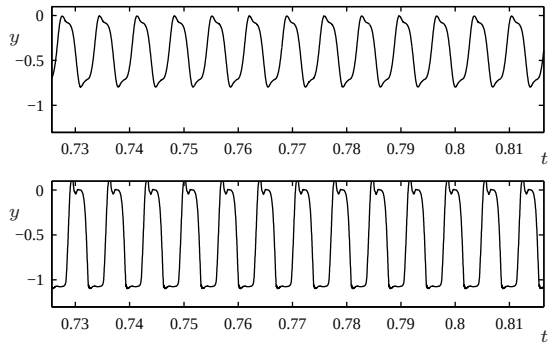

Figure 6: *Non-dimensional reed displacement y, for a clarinetlike configuration, of parameters as given in the caption to Figure 5, and with a bore profile as shown in Figure 5(b). The parameters for the collision term in* (4) *are chosen as $\omega_1 = 632$, and the nonlinearity exponent is $\alpha = 4$. In (a), the input is a steady nondimensional mouth pressure of $p_{\rm m} = 0.013$, and in (b), $p_{\rm m} = 0.02$.*

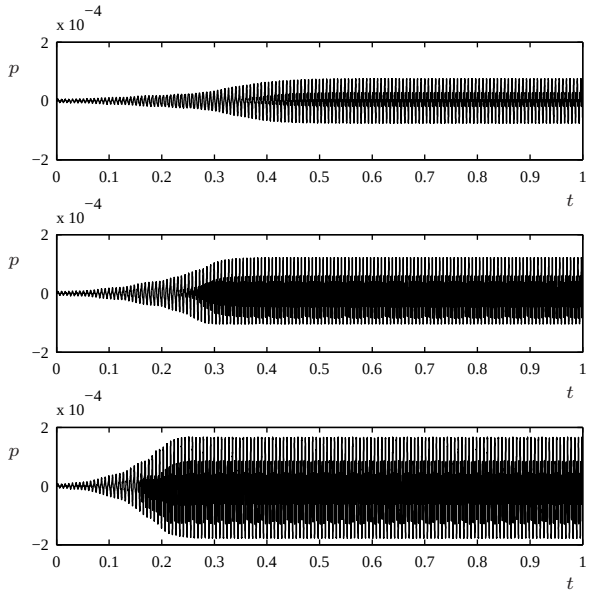

Figure 7: *Non-dimensional output pressure, for the wind model of parameters given in the caption to Figure 5, and using the clarinetlike bore profile shown in Figure 5(b). Top, with a nondimensional mouth pressure of $p_{\rm m} = 0.0134$, center, with $p_{\rm m} = 0.0148$, and bottom, with $p_{\rm m} = 0.0168$.*

5.1. Bore Profiles

It is particularly simple, in the direct FD framework, to alter the bore profile—the function $S(x)$ may be set arbitrarily, and once set, values of the function are used, without further calculations (as of scattering coefficients or impedances) in the simulation. It is thus straightforward to experiment with bore profiles which may differ substantially from, e.g., those which lead to efficient waveguide realizations. See Figure 5. (One must beware, however, that for extreme variations in the cross-sectional area, Webster's equation itself fails to be a good model of the tube dynamics.) In particular, computational effort is independent of the choice of bore profile.

5.2. Reed Beating

As an example of typical phenomena generated by such a model, consider the perceptually important reed-beating effect, as illustrated in Figure 6. In particular, note that the nondimensional reed displacement takes on values < -1; the extent of such "penetration" may be controlled through the choice of ω_1 and α, but the general results are in agreement with other published results (see, e.g., [41]).

5.3. Onset Times

As another example, the variation in onset times for notes as a function of mouth pressure, characteristic of wind instruments, is shown in Figure 7.

5.4. Time-varying Reed Equilibrium Displacement

When the equilibrium reed displacement H_0 is allowed to vary slightly, and at sub-audio rates (as in a typical wind instrument gesture), variations in timbre result—see Figure 8.

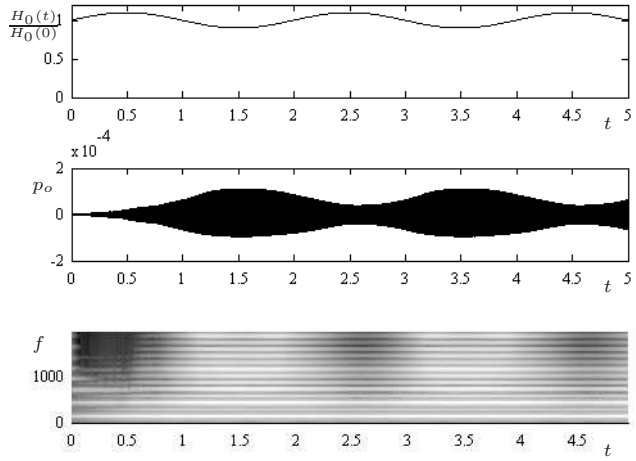

Figure 8: *Top: relative variation in reed equilibrium displacement $H(t)/H_0$. Middle: output pressure waveform (non-dimensional), and bottom, its spectrogram. The model is of parameters as described in the caption to Figure 5, and the input waveform is a constant with $p_{\rm m} = 0.013$. Scheme* (11) *is used, at a sample rate of 48 kHz.*

5.5. Tonehole Openings

Like other physical modeling synthesis methods, the FD tonehole model in (20) allows for changes in pitch, through time varia-

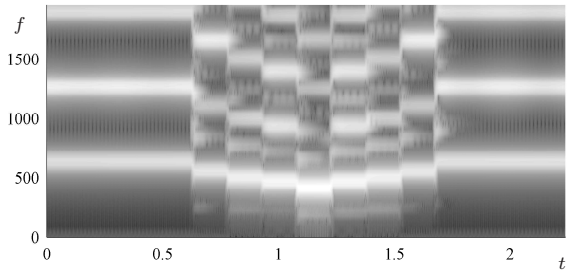

Figure 9: *Spectrogram of output pressure, for gesture in an instrument of conical bore. Five toneholes are tuned approximately to a minor scale.*

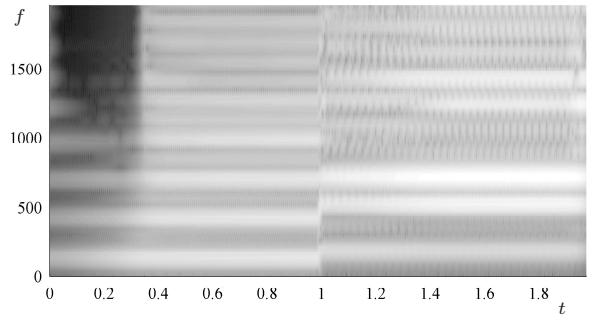

Figure 10: *Spectrogram of output pressure, for the wind model of parameters given in the caption to Figure 5, and using the clarinet-like bore profile shown in Figure 5(b), with a tonehole located at* $x_{\mathrm{T}} = 0.6$*, with parameters* $S_{\mathrm{T}} = 0.1644$*,* $\xi = 0.0075$*, and* $\xi_{\mathrm{e}} = 0.0134$*. The tonehole is opened, over a duration of 10 ms, at time* $t = 1$ *s.*

tion in the parameter ϕ, which specifies a state between open and closed—see Figure 9, which is generated using a saxophone-like model, with a series of toneholes.

5.6. Squeaks and Multiphonics

A variety of multiphonics may be generated though judicious placement of toneholes. If, for instance, a single tonehole is opened a good distance away from the bell, one is likely to generate a sound with a multiphonic character, exhibiting, perhaps, distinct sounding pitches, and a sub-audio rate time-varying amplitude envelope—see Figure 10, illustrating such a “warbling" effect. The space of such sounds, as any wind player will know, is very large indeed, and will depend on mouth pressure, the rate at which the hole is opened or closed, in addition to the particulars of tonehole placement and geometry.

6. CONCLUSION

Perhaps the greatest advantage of a fully discrete formulation is fidelity to the physics of the continuous time/space model itself; as a result, many issues which appear in more efficient designs, such as “lumping" of impedances, fractional delay interpolation, etc., may be sidestepped. Another advantage is extensibility—see below for some examples. The greatest disadvantage is computational cost, which is, in fact, quite small by today’s standards, though certainly higher than that of, e.g., a waveguide model.

There are many ways in which the FD wind model here could be extended. Several are in progress, and have not been discussed in this short paper—in particular, there is a simple extension to “blown open" brass-like instruments which is nearly trivial, involving only a single change in polarity of the pressure difference Δp in the model. Another obvious step is the porting of such an algorithm to a real time environment such as Max/MSP [42] or csound [43]—as noted earlier, a real time implementation is easily possible, and such developments are under way.

Other extensions are also possible. The fully discrete FD approach is very well suited to an extension to nonlinear 1D wave propagation—the linearity hypothesis is probably sufficient for reed instruments, and brass instruments under moderate amplitude excitation, though nonlinear effects do appear at high amplitudes in instruments such as the trombone [44], and have indeed been modelled in synthesis applications [45, 46]. Fully discrete methods in computing shock wave solutions have a very long history in mainstream fluid dynamics applications—see, e.g., the text by Hirsch [47], or the classic article by Sod [48], and, especially, the text by Leveque [49], which is concerned with finite volume methods in the context of nonlinear fluid dynamics applications. The introduction of loss in the acoustic tube, however, is in some ways more problematic. Often, loss in the boundary layer of a tube is modelled in the frequency domain—when transformed back to the time domain, one arrives at a PDE involving fractional derivatives, which can cause immense difficulty numerically, though discrete models of loss have been examined in great detail, in the scattering context, by various authors [50, 51]. Finally, the model described here is generally valid when bore radius is small compared to audio wavelengths, and when its spatial variation is not too great. In such cases, one may need to resort to models of wave propagation incorporating higher modes, and possibly mode conversion. In the fully discrete case, one could employ a three-dimensional model of the tube, with a very coarse grid approximation in the transverse direction [16], though one must beware the effects of numerical dispersion, which can be extreme in coordinate systems other than Cartesian.

7. REFERENCES

[1] J. O. Smith III, “Efficient simulation of the reed-bore and bow-string mechanisms,” in *Proceedings of the International Computer Music Conference*, The Hague, The Netherlands, October 1986, pp. 275–280.

[2] G. Scavone, *An Acoustic Analysis of Single-Reed Woodwind Instruments with an Emphasis on Design and Performance Issues and Digital Waveguide Techniques*, Ph.D. thesis, Department of Music, Stanford University, 1997.

[3] M. van Walstijn and D. Campbell, “Discrete-time modeling of woodwind instrument bores using wave variables,” *Journal of the Acoustical Society of America*, vol. 113, no. 1, pp. 575–585, 2003.

[4] M. van Walstijn, “Wave-based simulation of wind instrument resonators,” *IEEE Signal Processing Magazine*, vol. 24, no. 2, pp. 21–31, 2007.

[5] A. Fettweis, "Wave digital filters: Theory and practice," *Proceedings of the IEEE*, vol. 74, no. 2, pp. 270–327, 1986.

[6] S. Bilbao, J. Bensa, and R. Kronland-Martinet, "The wave digital reed: A passive formulation," in *Proceedings of the COST-G6 Digital Audio Effects Conference*, London, UK, September 2003, pp. 225–230.

[7] M. van Walstijn and G. Scavone, "The wave digital tonehole model," in *Proceedings of the International Computer Music Conference*, Berlin, Germany, August 2000, pp. 465–468.

[8] P. Guillemain, "A digital synthesis model of double-reed wind instruments," *EURASIP Journal of Applied Signal Processing*, vol. 7, pp. 990–1000, 2004.

[9] F. Avanzini and D. Rocchesso, "Efficiency, accuracy, and stability issues in discrete time simulations of single reed instruments," *Journal of the Acoustical Society of America*, vol. 111, no. 5, pp. 2293–2301, 2002.

[10] M. van Walstijn and F. Avanzini, "Modeling the mechanical response of the reed-mouthpiece-lip system of a clarinet. Part II: A lumped model approximation," *Acta Acustica united with Acustica*, vol. 93, no. 3, pp. 435–446, 2007.

[11] F. Avanzini and M. van Walstijn, "The mechanical response of the reed-mouthpiece-lip system of a clarinet. Part I. A one-dimensional distributed model," *Acta Acustica united with Acustica*, vol. 90, no. 3, pp. 537–547, 2004.

[12] M. McIntyre, R. Schumacher, and J. Woodhouse, "On the oscillations of musical instruments," *Journal of the Acoustical Society of America*, vol. 74, no. 5, pp. 1325–1345, 1983.

[13] K. van den Doel and U. Ascher, "Real-time numerical solution of websters equation on a non-uniform grid," *IEEE Transactions on Audio, Speech and Language Processing*, vol. 16, no. 6, pp. 1163–1172, 2008.

[14] M. Portnoff, "A quasi-one-dimensional digital simulation for the time-varying vocal tract," M.S. thesis, Massachusetts Institute of Technology, 1973.

[15] C. Nederveen, "Influence of a toroidal bend on wind instrument tuning," *Journal of the Acoustical Society of America*, vol. 104, no. 3, pp. 1616–1626, 1998.

[16] D. Noreland, "A numerical method for acoustic waves in horns," *Acustica united with Acustica*, vol. 88, no. 4, pp. 576–586, 2002.

[17] S. Bilbao, "Direct simulation for wind instrument synthesis," in *Proceedings of the 11th International Digital Audio Effects Conference*, Espoo, Finland, September 2008, pp. 145–152.

[18] S. Bilbao, *Numerical Sound Synthesis: Finite Difference Schemes and Simulation in Musical Acoustics*, John Wiley and Sons, Chichester, UK, 2009, In Press.

[19] P. Morse and U. Ingard, *Theoretical Acoustics*, Princeton University Press, Princeton, New Jersey, 1968.

[20] A. Benade and E. Jansson, "On plane and spherical waves in horns with nonuniform flare I. Theory of radiation, resonance frequencies, and mode conversion," *Acustica*, vol. 31, no. 2, pp. 80–98, 1974.

[21] N. Fletcher and T. Rossing, *The Physics of Musical Instruments*, Springer-Verlag, New York, New York, 1991.

[22] L. Rabiner and R. Schafer, *Digital Processing of Speech Signals*, Prentice-Hall, Englewood Cliffs, New Jersey, 1978.

[23] J. Kelly and C. Lochbaum, "Speech synthesis," in *Proceedings of the Fourth International Congress on Acoustics*, Copenhagen, Denmark, 1962, pp. 1–4, Paper G42.

[24] A. Chaigne and A. Askenfelt, "Numerical simulations of struck strings. I. A physical model for a struck string using finite difference methods," *Journal of the Acoustical Society of America*, vol. 95, no. 2, pp. 1112–1118, 1994.

[25] J. Kergomard P. Guillemain and T. Voinier, "Real-time synthesis of clarinet-like instruments using digital impedance models," *Journal of the Acoustical Society of America*, vol. 118, no. 1, pp. 483–494, 2005.

[26] J. Kergomard, "Elementary considerations on reed-instrument oscillations," in *Mechanics of Musical Instruments, Lecture notes CISM*, Hirschberg et al., Ed. Springer, New York, New York, 1995.

[27] T. Tachibana and K. Takahashi, "Sounding mechanism of a cylindrical pipe fitted with a clarinet mouthpiece," *Progress of Theoretical Physics*, vol. 104, no. 2, pp. 265–288, 2000.

[28] J.-P. Dalmont, J. Gilbert, and S. Ollivier, "Nonlinear characteristics of single-reed instruments: Quasistatic volume flow and reed opening characteristics," *Journal of the Acoustical Society of America*, vol. 114, no. 4, pp. 2253–2262, 2003.

[29] J. Backus, "Small vibration theory of the clarinet," *Journal of the Acoustical Society of America*, vol. 35, pp. 305–313, 1963.

[30] M. Atig, J.-P. Dalmont, and J. Gilbert, "Termination impedance of open-ended cylindrical tubes at high sound pressure level," *Comptes Rendus Mécanique*, vol. 332, pp. 299–304, 2004.

[31] V. Belevitch, *Classical Network Theory*, Holden Day, San Francisco, California, 1968.

[32] J. Strikwerda, *Finite Difference Schemes and Partial Differential Equations*, Wadsworth and Brooks/Cole Advanced Books and Software, Pacific Grove, California, 1989.

[33] R. Courant, K. Friedrichs, and H. Lewy, "Über die partiellen Differenzengleichungen de mathematischen Physik," *Mathematische Annalen*, vol. 100, pp. 32–74, 1928.

[34] G. R. Shubin and J. B. Bell, "A modified equation approach to constructing fourth order methods for acoustic wave propagation," *SIAM Journal of Scientific and Statistical Computing*, vol. 8, pp. 135–51, 1987.

[35] V. Välimäki and M. Karjalainen, "Implementation of fractional delay waveguide models using allpass filters," in *Proceedings of the IEEE International Conference on Acoustics, Speech, and Signal Processing*, Detroit, Michigan, May 1995, pp. 8–12.

[36] S. Bilbao, *Wave and Scattering Methods for Numerical Simulation*, John Wiley and Sons, Chichester, UK, 2004.

[37] D. Keefe, "Theory of the single woodwind tone hole," *Journal of the Acoustical Society of America*, vol. 72, no. 3, pp. 676–687, 1982.

[38] D. Keefe, "Experiments on the single woodwind tone hole," *Journal of the Acoustical Society of America*, vol. 72, no. 3, pp. 688–699, 1982.

[39] D. Keefe, "Woodwind air column models," *Journal of the Acoustical Society of America*, vol. 88, no. 1, pp. 35–51, 1990.

[40] E. Ducasse, "A physical model of a single reed wind instrument, including actions of the player," *Computer Music Journal*, vol. 27, no. 1, pp. 59–70, 2003.

[41] D. Keefe, "Physical modeling of wind instruments," *Computer Music Journal*, vol. 16, no. 4, pp. 57–73, 1992.

[42] D. Zicarelli, "How I learned to love a program that does nothing," *Computer Music Journal*, vol. 26, no. 4, pp. 44–51, 2002.

[43] R. Boulanger, Ed., *The csound Book: Perspectives in Software Synthesis, Sound Design, Signal Processing, and Programming*, MIT Press, Cambridge, Massachusetts, 2001.

[44] A. Hirschberg, J. Gilbert, R. Msallam, and A. Wijnands, "Shock waves in trombones," *Journal of the Acoustical Society of America*, vol. 99, no. 3, pp. 1754–1758, 1996.

[45] R. Msallam, S. Dequidt, S. Tassart, and R Caussé, "Physical model of the trombone including nonlinear propagation effects. Application to the sound synthesis of loud tones," *Acta Acustica United with Acustica*, vol. 86, pp. 725–736, 2000.

[46] C. Vergez and X. Rodet, "A new algorithm for nonlinear propagation of sound wave: Application to a physical model of a trumpet," *Journal of Signal Processing*, vol. 4, pp. 79–88, 2000.

[47] C. Hirsch, *Numerical Computation of Internal and External Flows*, John Wiley and Sons, Chichester, UK, 1988.

[48] G. Sod, "A survey of several finite difference methods for systems of nonlinear hyperbolic conservation laws," *Journal of Computational Physics*, vol. 27, no. 1, pp. 1–31, April 1978.

[49] R. Leveque, *Finite Volume Methods for Hyperbolic Problems*, Cambridge Texts in Applied Mathematics, Cambridge, UK, 2002.

[50] T. Hélie and D. Matignon, "Diffusive representations for the analysis and simulation of flared acoustic pipes with viscothermal losses," *Mathematical Models and Methods in Applied Sciences*, vol. 16, no. 4, pp. 503–536, 2006.

[51] R. Mignot, T. Hélie, and D. Matignon, "State-space representations for digital waveguide networks of lossy flared acoustic pipes," Submitted to the International Conference on Digital Audio Effects, 2009.